Fig S1
Stereoview of the mFo-dFc electron density map (green) contoured at 2.0 σ level for the DSA molecule omitted for calculation and shown in ball-and-stick mode.

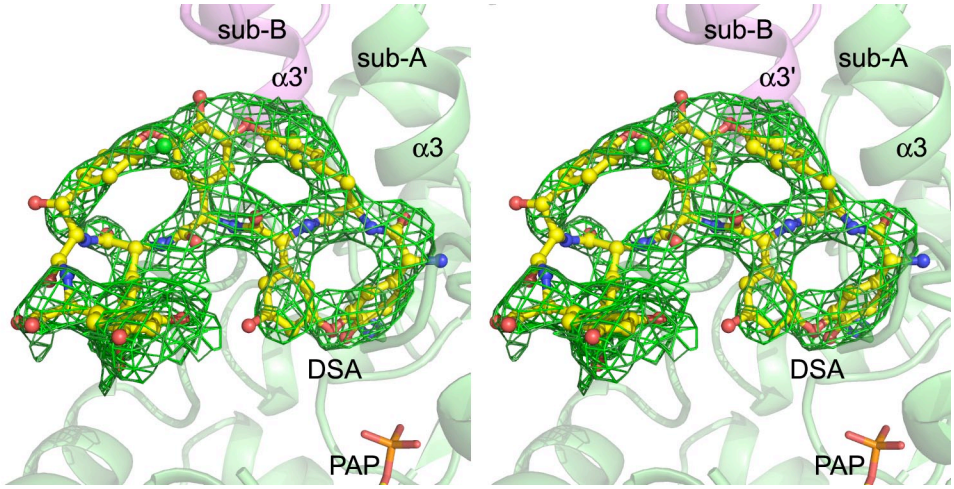

Fig S2
Active site details. The modeled PAPS (carbon in salmon) molecule is superposed onto PAP (carbon in orange) in the crystal structure. H-bonds are shown in black dashed lines.

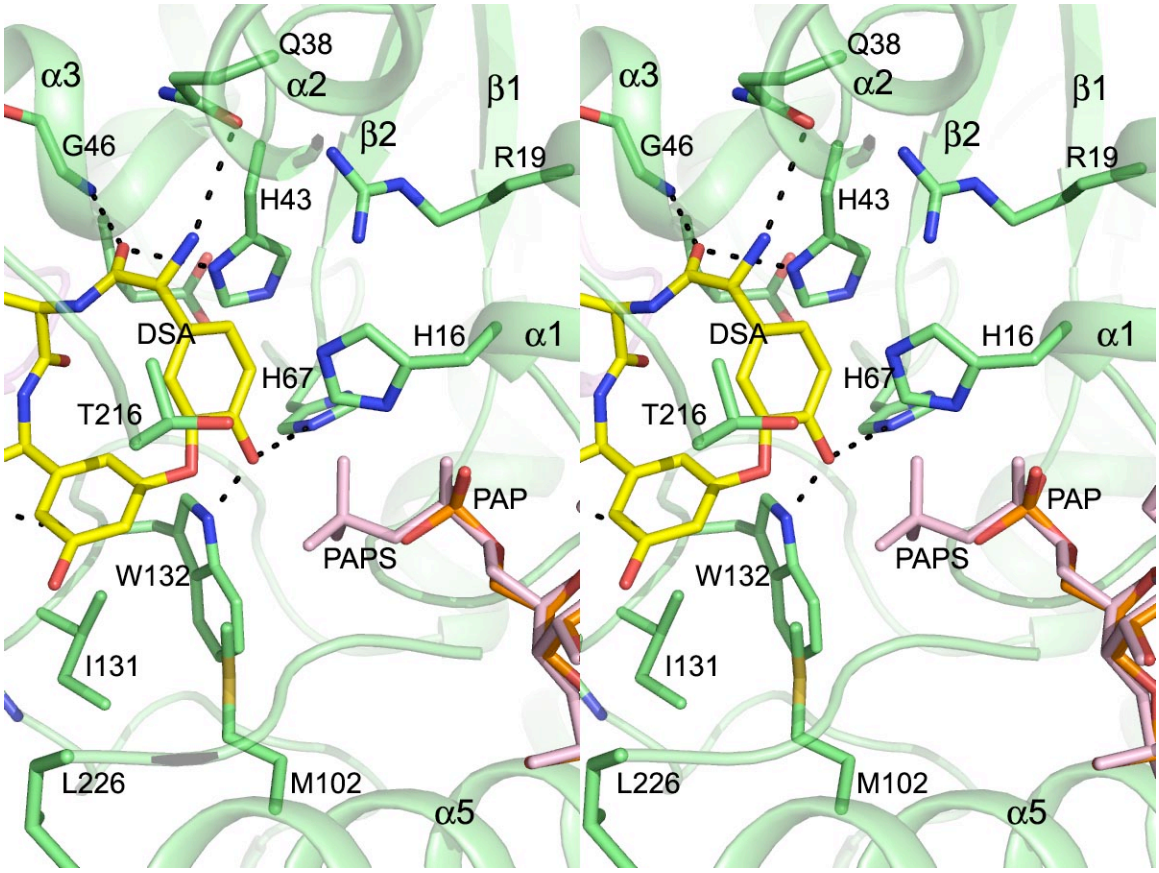

Fig S3
Slight conformational changes of StaL upon binding of the DSA molecule. The carbon atoms of the residues in the StaL-PAP-DSA complex are colored in light green (sub-A) and magenta (sub-B). The changes mainly occur on residues R49 and R130 (carbon in white for the StaL-PAP complex).

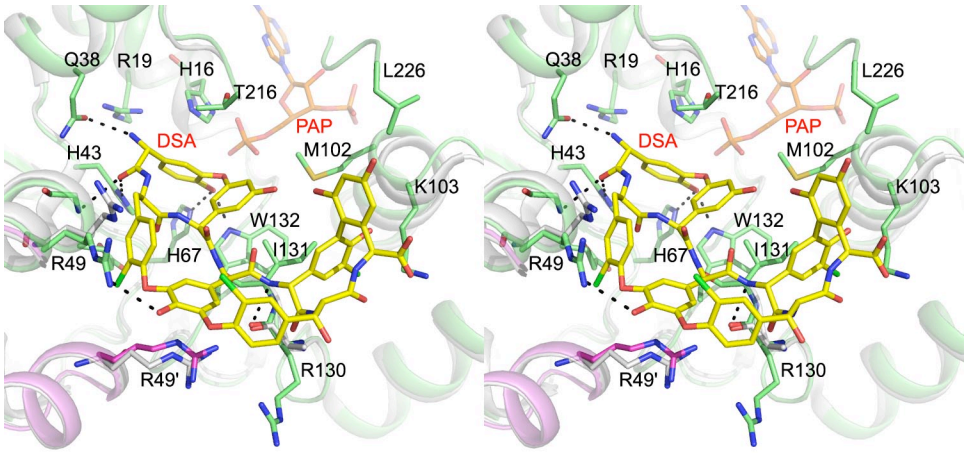

Fig S4
The segment L226-V229 is sandwiched between helices α5 and α12. This segment stabilizes the PAP binding by van der Waals contacts. The H-bonding interactions between the E205 carboxylate sidechain and the amide groups of F228 and V229 are shown in black dashed lines.

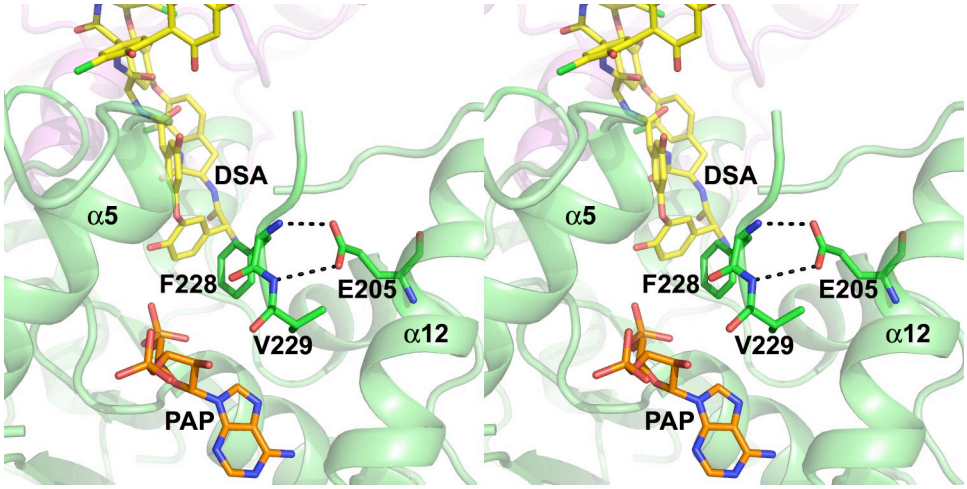

Fig S5
Surface representation of involvement of both subunits in binding one DSA molecule.

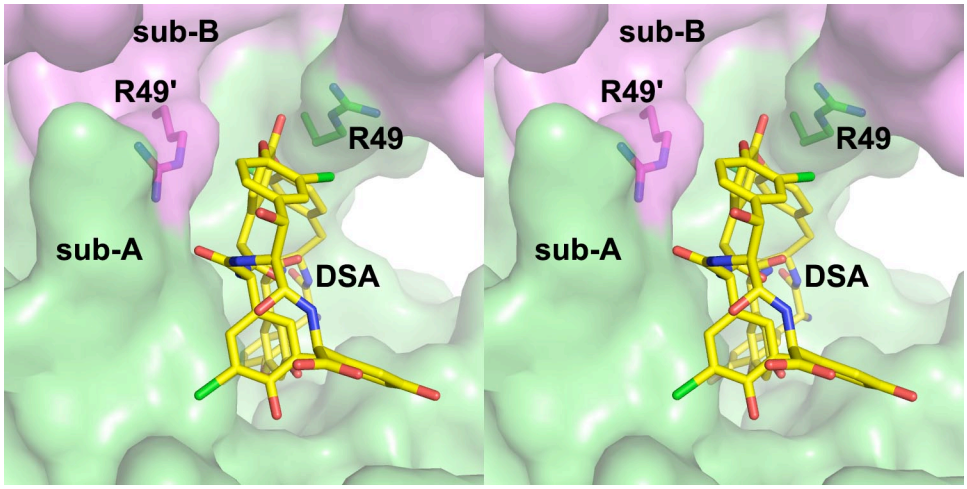

Fig S6
The relative positioning of R130 at the interface of two subunits. Ordering of R130 upon DSA binding in subunit A (in green) of the StaL-PAP-DSA ternary complex may displace the segment 210-216 (loop L3 and the C-terminal of α12) from its initial position in subunit B due to their proximity, which subsequently decreases the affinity of subunit B (in magenta) for PAP binding. A copy of subunit A (in white) is superposed onto subunit B showing the relative positioning of R130, the loop (indicated by red arrow) and α12, as well as the PAP molecule.

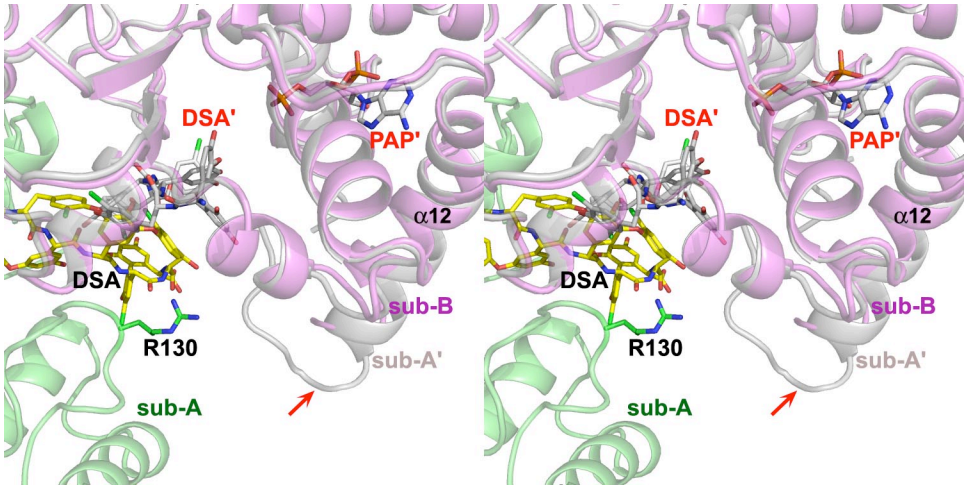

Fig S7
Superposition of the aglycone portions of vancomycin (carbon in cyan, PDB 1FVM) and ristocetin A (carbon in green, the CCDC deposition number 718620), both in complexes with the cell-wall precursor (carbons of the cell-wall precursor are in white and orange for vancomycin and ristocetin A complexes, respectively). This indicates that the aglycone portions of both vancomycin and teicoplanin classes adopt a similar cup-shape and maintain almost identical interactions with the cell-wall precursor by their concave sides . The H-bonds are shown in dash lines.

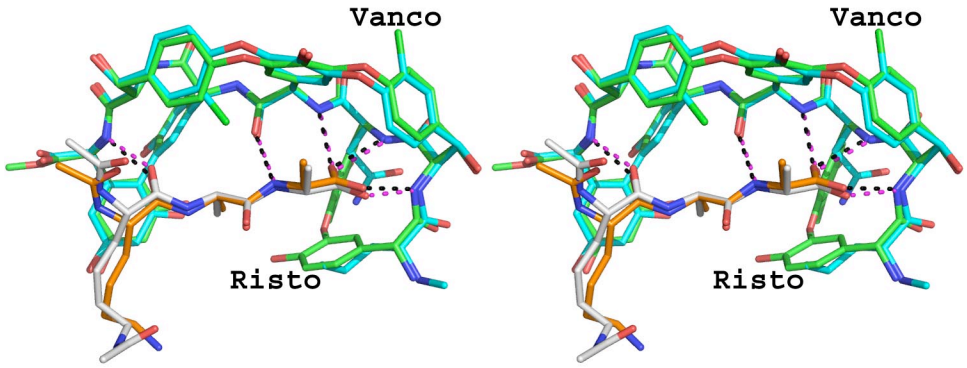

Fig S8
Stereoview of the superposition of A40926 aglycone (carbon in magenta) and the DSA molecule showing drastic differences in the conformations of res 1-3.

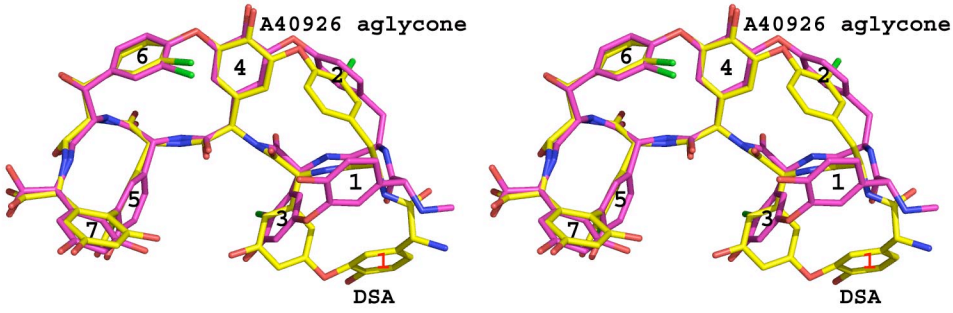

Fig S9
Superposition of the DSA molecule (carbon in yellow) and the aglycone portion of teicoplanin (carbon in cyan, PDB 2XAD, chain H) revealing almost identical conformation.

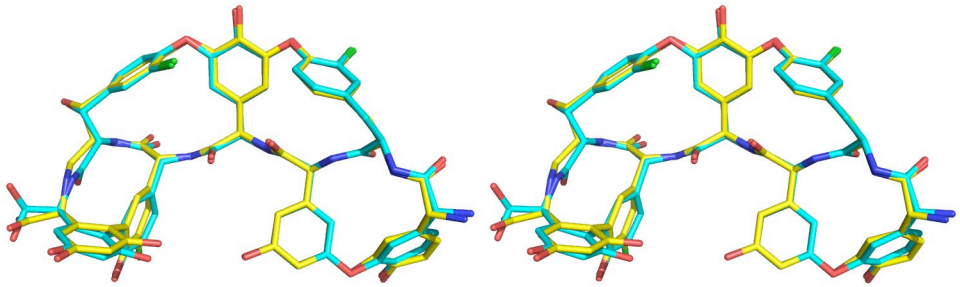

Fig S10
Superposition of the cup-shaped teicoplain aglycone (carbon in salmon) onto the teicoplanin molecule (carbon in cyan) bound to the deacetylase Orf2* (PDB 2XAD, chain D) showing why the aglycone portion of the teicoplanin needs to be flattened to avoid the steric clashes with the narrow entry tunnel (the substrate binding site).

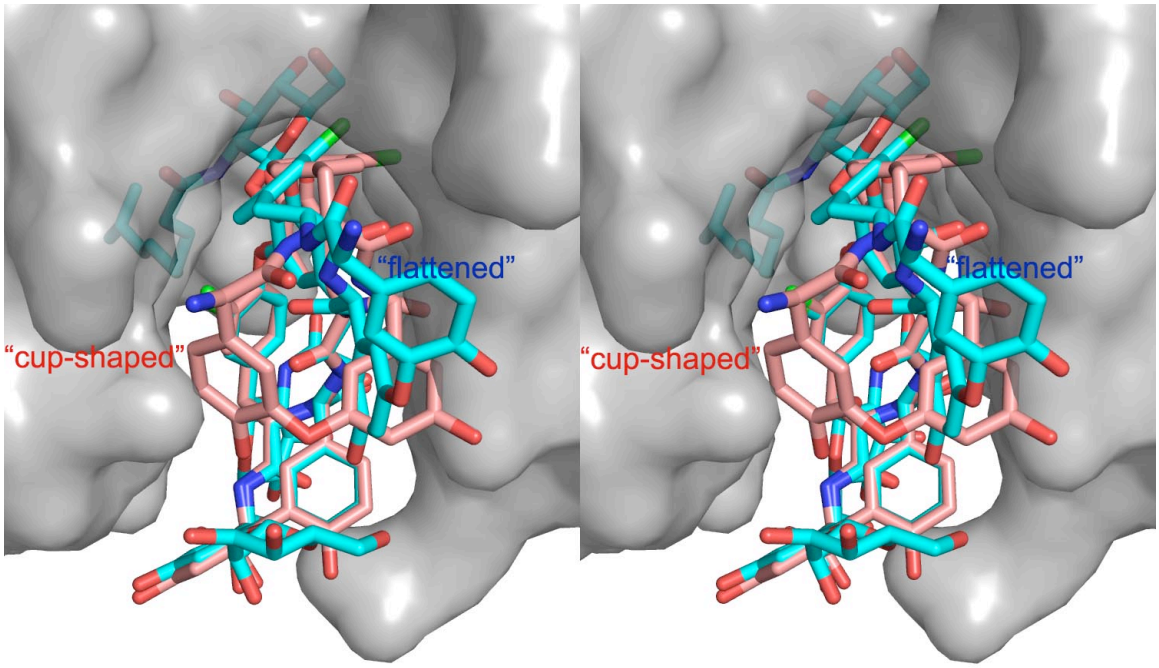

Fig S11
Superposition of the aglycone portion of vancomycin (carbon in cyan, PDB 1FVM) onto desvancosaminyl vancomycin (carbon in white) bound to the vancosaminyltransferase GtfD (PDB 1RRV) showing that residues 1-3 of the scaffold undergo conformational changes to avoid the potential steric conflicts with the surrounding residues (carbon in yellow).

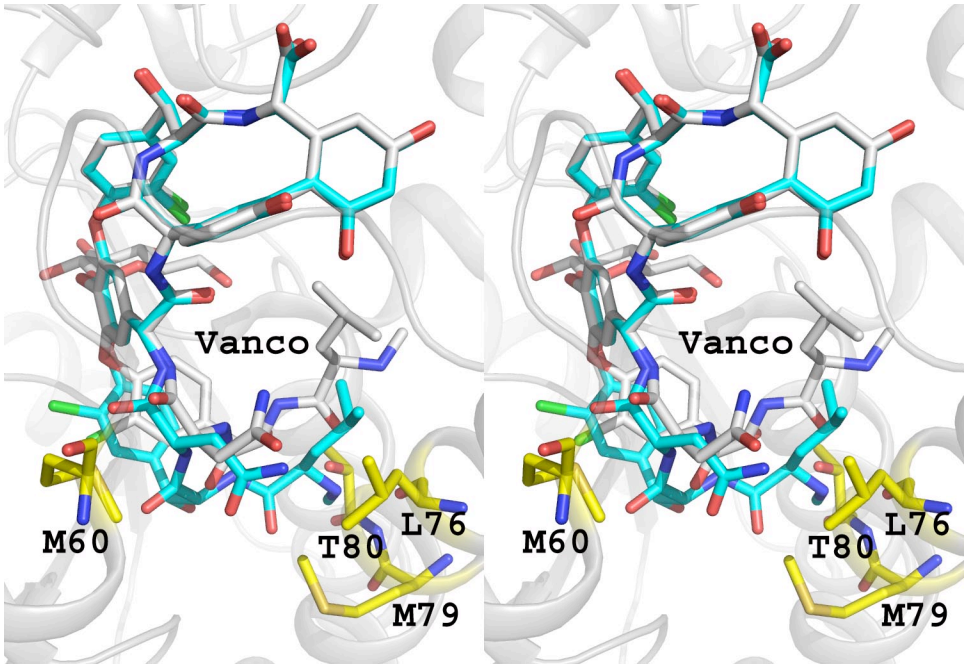

Fig S12
Superposition of the Teg12 (PDB 3MGB, in blue) and Teg14 (PDB 3NIB, in salmon) structures onto the StaL-PAP-DSA ternary complex (green). The three variable regions (V1, V2 and V3) as well as the loop α5/α6 are indicated.

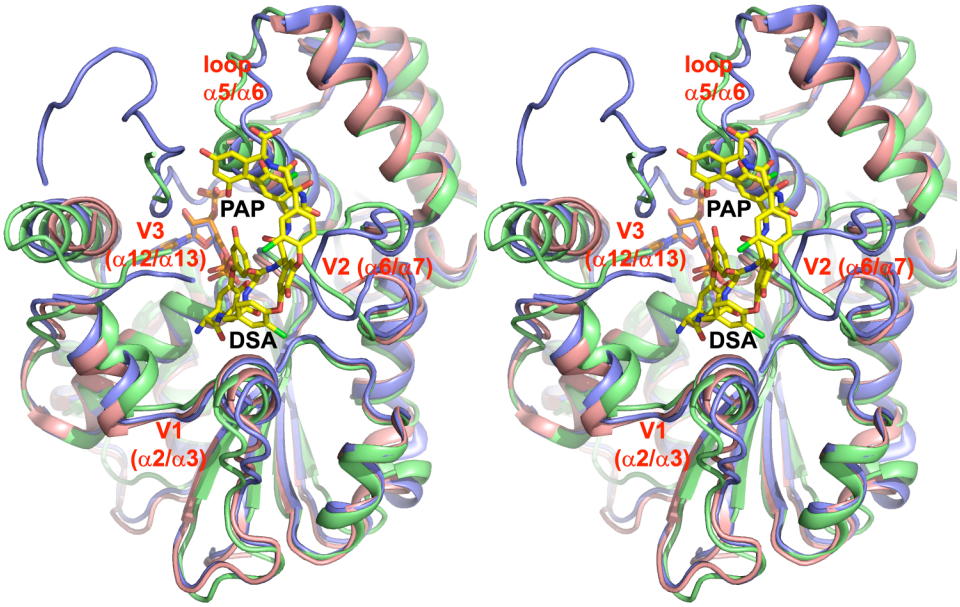

Fig S13

Docking of a virtual hybrid GPA molecule with DSA as its scaffold onto the StaL substrate binding pocket. In this energy-minimized model refined with the AMBER force field (Hornak et al., 2006; Wang et al., 2004), StaL is shown as translucent surface with subunit A in green and B in magenta. The scaffold is labeled (residues 1-7) and shown as capped sticks with carbon atoms in white, and the added substituents (labeled R1-R6, details in the main text) are shown as ball-and-stick models with carbon atoms in cyan. The distance for nucleophilic attack of phenolic oxygen at residue 1 of GPA to the sulfur atom of PAPS is 3.1 Å and is indicated by a dashed line. (a) and (b) are two different views.

(Hornak V, Abel R, Okur A, Strockbine B, Roitberg A, & Simmerling C. (2006) Comparison of multiple Amber force fields and development of improved protein backbone parameters. *Proteins* 65:712– 725.

Wang J, Wolf RM, Caldwell JW, Kollman PA, & Case DA. (2004) Development and testing of a general Amber force field. *J. Comput. Chem.* 25:1157-1174.)

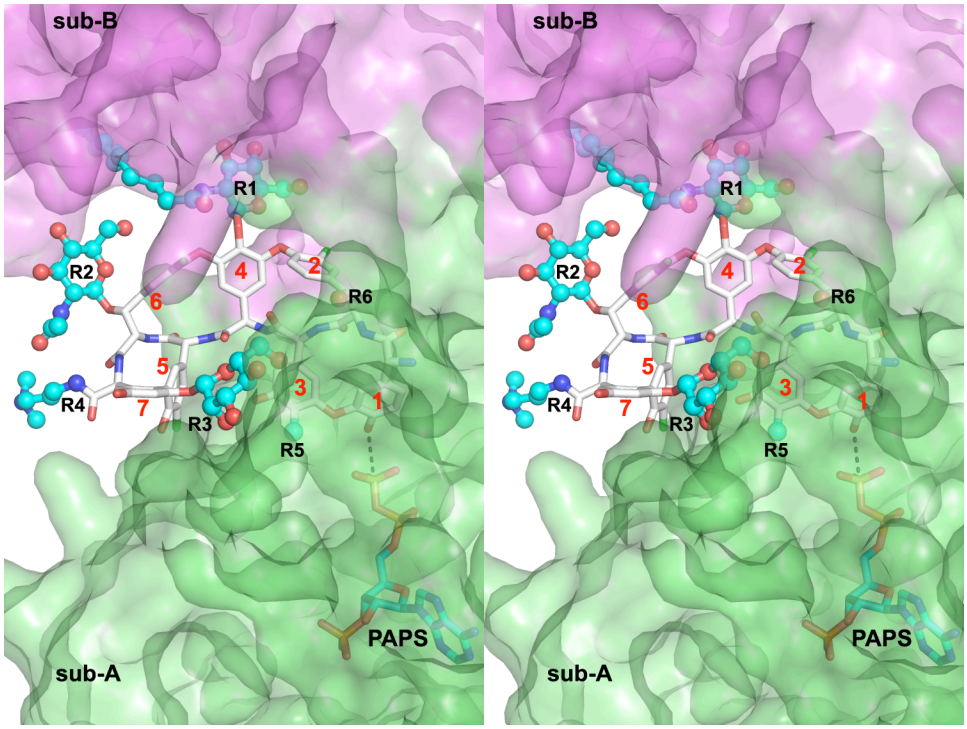

a

b

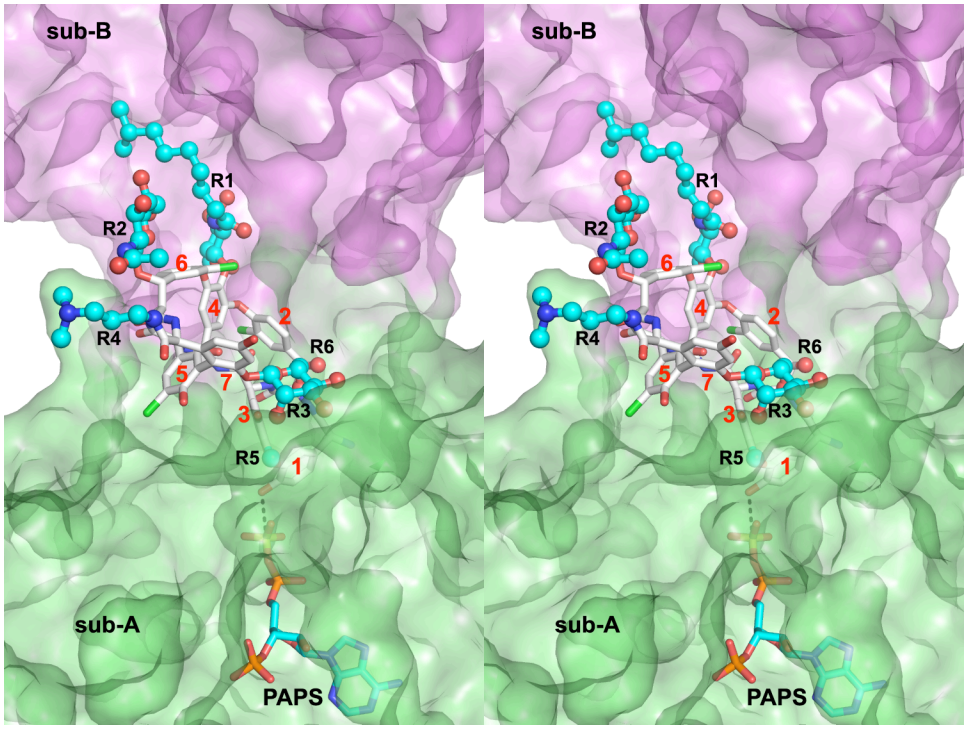
sub-B
R1
R2
6
4
2
R4
R6
5
7
3
R3
R5
1
sub-A
PAPS
sub-B
R1
R2
6
4
2
R4
R6
5
7
3
R3
R5
1
sub-A
PAPS